Automatic LADAR Calibration Methods using Geometric Optimization

B. Guerreiro*, C. Silvestre* and P. Oliveira*
Instituto Superior Técnico, Institute for Systems and Robotics
Av. Rovisco Pais, 1, 1049-001 Lisboa, Portugal
{bguerreiro,cjs,pjcro}@isr.ist.utl.pt

***Abstract*— This paper proposes an estimation algorithm for the determination of attitude installation matrix for laser detection and ranging systems (LADAR) mounted onboard autonomous vehicles, without requiring any prior knowledge on the terrain where the calibration mission is performed. The use of autonomous vehicles equipped with LADAR systems to conduct fully automatic surveys of terrain, infrastructures, or just to navigate safely in unknown environments, motivates the research on increasingly precise LADAR data acquisition and processing algorithms, for which the determination of the correct installation matrix is critical. The proposed methods rely on the minimization of the errors between several acquired data sets, by comparing each measured data set and a surface representation of the others. This error functional is minimized resorting to optimization tools for Riemannian manifolds enabling direct estimation of the installation matrix on the group of special orthogonal matrices SO(3). The proposed technique is extensively tested using simulated LADAR data sets under realistic acquisition conditions.**

I. Introduction

Laser Detection and Ranging (LADAR) systems technology is nowadays widely used by the robotics and the remote sensing research communities. The development of airborne laser ranging sensors started in the 1970s in North America, mainly for topographic applications. Later, with the development of affordable Inertial Navigation System (INS) and Global Positioning System (GPS) units, other applications captured the attention of the research community, such as monitoring ice sheets [1] or measuring canopy heights [2]. The robotics research community is nowadays employing autonomous vehicles equipped with LADARs to perform automatic acquisition and 3-D reconstruction of terrain, buildings, large infrastructures or using this information to safely navigate through unknown environments [3], [4]. For all these applications the data accuracy is essential. However, there are several sources of inaccuracy that can lead to considerable nonlinear reconstruction errors, for instance, an airborne LADAR acquiring terrain elevation 1 km above the ground, with 0.01 rad of roll mounting bias will generate points with an error of 10 m, with a planar terrain (otherwise nonlinear distortions will appear). Thus, the calibration of these errors, specially the attitude installation bias, is fundamental to meet the desired accuracy requirements.

In most applications the LADAR system is installed in a platform equipped with an INS/GPS unit, which provides position and attitude data that, together with the relative distance measured by the LADAR, enables the reconstruction of the surrounding environment. Conversely to other calibration procedures that require particular terrain features and/or specific vehicle trajectories in order to calibrate a subset of the parameters [5], in the proposed method the only information required for LADAR calibration are clouds of 3-D points. Thus, there is no matching information between points and also no previous knowledge on the terrain where the calibration mission is performed. For instance, a standard procedure in the literature for laser calibration would be to fly over a known flat surface while performing pitch and roll maneuvers, separately, which enables the calibration of only these two parameters. Since there is no direct technique to compare the measured data set with the corresponding real points, one approach is to compare the measured data set with a representation of the real surface [6]. This technique is used in [7] with the linearization of the error model to obtain a Gauss-Helmert model, which is used to estimate the installation bias. In [8], this approach was generalized using nonlinear and geometric optimization techniques, but still shares the main difficulty for practical implementation: a known calibration surface is needed to compare with the acquired data. In the present work, no a priori knowledge on any surface is required as the proposed method compares directly at least two sets of acquired data. Nonetheless, there should be enough information on the calibration surface and vehicle trajectories to enable the full attitude installation bias calibration. The comparison of each set of acquired data, or cloud of points, is compared with a surface approximation of all the remaining sets by measuring the minimum distance of each point to the approximated surfaces. The intuition behind this approach is that there should be only one installation matrix that justifies all the acquired sets of data.

The estimation problem is formulated within the scope of maximum likelihood (ML) theory [9], allowing the formulation of the calibration problem as an optimization problem. The real valued cost functional to be minimized is defined by the summation of the errors between each measured data set and the surface approximation of the other sets. The optimization approach resorts to optimization tools on Riemannian manifolds, enabling the use of Gradient and

*This work was partially supported by Fundação para a Ciência e a Tecnologia (ISR/IST pluriannual funding) and project AIRTICI from ADI through the POS Conhecimento Program that includes FEDER funds, and by the project PTDC/HIS-ARQ/103227/2008 AMMAIA project. The work of Bruno Guerreiro was supported by the PhD Student Grant SFRH/BD/21781/2005 from the Portuguese FCT POCTI programme.

Newton methods to directly estimate the installation matrix on the group of special orthogonal matrices SO(3) [10], [11]. This approach can also use a line search algorithm, such as the the Wolfe rule to compute the step size [12], nonetheless, there exists an exact computation of the step size algorithm within SO(3), [13]. The proposed calibration technique is tested using simulated data sets to assess its performance and limitations. The paper is organized as follows: Section II introduces the reconstruction error model, a ML formulation is proposed, and the calibration problem is written as a nonlinear optimization problem. Section III introduces the Riemannian optimization tools used to solve the problem. Simulation results and an in-depth discussion of the algorithm presented in Section IV. Finally, in Section V the main conclusions are offered and directions for further work are outlined.

II. Reconstruction Error Model

In this section the reconstruction error model and the calibration problem are introduced. This calibration problem is formulated in such a way that the use of a known calibration surface is avoided, introducing the idea of comparing different clouds of the same terrain with each other. In the following three subsections, the point reconstruction, the cloud-to-cloud comparison, and the calibration problem are introduced.

A. Point Reconstruction

The point reconstruction model describes the transformation of the LADAR raw data, composed by a range measurement and an incidence angle, into 3-D points. The following coordinate frames are introduced: $\{I\}$ as the inertial frame; $\{ins\}$ as INS/GPS frame; $\{l\}$ as the LADAR frame, with origin at the laser's firing point and z-axis indicating the zero scanning angle; $\{lb\}$ as the laser beam frame, with origin at the firing point, y-axis collinear with that of frame $\{l\}$ and z-axis oriented opposite to the direction of the laser beam. These frames and the connections between them are depicted in Fig. 1. Each measurement k is defined as the

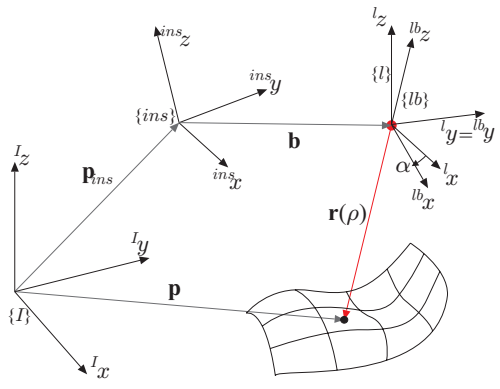

Fig. 1. Ladar coordinate frames

distance between the laser firing point and the laser hit point, ρ_k, and by the angular position of the laser beam, α_k, that is, the angle from $\{l\}$ to $\{lb\}$. Thus, it can easily be seen that the expression that transforms the LADAR measurement (ρ_k, α_k) into the reconstructed 3-D point $\mathbf{p}_k$, expressed in the inertial frame, is given by

$$\mathbf{p}_k = R_{ins_k}\left(R\, R_l\, R_{lb}(\alpha_k)\, \mathbf{r}(\rho_k) + \mathbf{b}\right) + \mathbf{p}_{ins_k}\ , \quad (1)$$

where R_{ins_k} is the platform attitude defined by the rotation from $\{ins\}$ to $\{I\}$, R_l is the known attitude mounting bias defined by the rotation from $\{l\}$ to $\{ins\}$, $R_{lb}(\alpha_k)$ is the rotation from $\{lb\}$ to $\{l\}$, that defines the laser beam rotation and is given by $R_{lb}(\alpha_k) = R_Y(\alpha_k)$, with $R_Y(.)$ standing for the rotation matrix about the y axis, $\mathbf{r}(\rho_k) = \begin{bmatrix} 0 & 0 & -\rho_k \end{bmatrix}'$, $\mathbf{p}_{ins_k}$ is the INS/GPS unit position expressed in $\{I\}$. The known position installation bias $\mathbf{b}$ denotes the laser firing point described in $\{ins\}$ and matrix R is the rotation matrix that defines the unknown attitude installation bias, which is an element of the group of special orthogonal matrices SO(3). Note that the position installation bias can be itself calibrated, however, it can be more accurately measured than the attitude installation bias. Let $\mathrm{M}(n,\mathbb{R}) = \{A : n \times n \text{ matrix with real entries}\}$ and the group of orthogonal matrices be defined as $\mathrm{O}(n) = \{U \in \mathrm{M}(n,\mathbb{R}) : U\,U' = I_{n\times n}\}$, then the group of special ortogonal matrices is $\mathrm{SO}(n) = \{R \in \mathrm{O}(n) : \det(R) = 1\}$.

B. Cloud-to-Cloud Comparison

Assume there are $n_c > 1$ clouds of points, $\mathcal{C}_i$ for $i = 1, \ldots, n_c$, resulting from different trajectories of the vehicle, such that the intersection of the laser data boundaries of each cloud projected into the xy-plane is nonempty. Each cloud is a set of n_{p_i} laser measurement points, $\mathcal{C}_i = \{\mathbf{p}_k^i\}$ for $k = 1, \ldots, n_{p_i}$, which represent a nonlinearly distorted sampling with noise of the real surface $\mathcal{S}_{\text{real}}$, and can be approximated by a piecewise surface $\mathcal{S}_i$, consisting in a set of n_{planes_i} planes. The fact that in this problem there is no correspondence between the points of the different clouds of points does not allow for a direct comparison. The proposed solution consists of comparing each cloud $\mathcal{C}_i$ with a surface approximation of all the remaining clouds, $\mathcal{S}_j$ for $j = 1, \ldots, n_c$ and $j \neq i$. For that purpose, it is assumed that the surface approximations can be represented by an elevation map, of the form $z = f_S(x, y)$, and that a piecewise surface defined by a set of n_{planes_i} can describe this function with arbitrarily small error, as $n_{planes_i} \to \infty$.

To compare the points of cloud $\mathcal{C}_i$ with the approximated surface of cloud $\mathcal{C}_j$, $\mathcal{S}_j$, each point is linked with the closest plane of $\mathcal{S}_j$ along its normal vector. Considering the set of planes that define $\mathcal{S}_j$, let the plane associated with the measurement k of $\mathcal{C}_i$ be defined by the plane equation $\mathbf{s}_k^{ij\prime}\, \mathbf{p}_k^i + {}^4s_k^{ij} = 0$, where $\mathbf{s}_k^{ij} = \begin{bmatrix} {}^1s_k^{ij} & {}^2s_k^{ij} & {}^3s_k^{ij} \end{bmatrix}' \in \mathbb{R}^3$ is the plane normal unitary vector and ${}^4s_k^{ij} \in \mathbb{R}$.

C. Calibration Problem

The calibration of a LADAR system can be formulated as the minimization of the error between each measured set of reconstructed points, $\mathcal{C}_i$, and the surface approximation of the remaining clouds, $\mathcal{S}_j$ for $j = 1, \ldots, n_c$ and $j \neq i$, subject to the LADAR model constraint. The error between each point

$\mathbf{p}_k^i$ and the associated plane of the control surface can be defined as $\mathbf{e}_k^{ij} = \mathbf{p}_{0_k}^{ij} - \mathbf{p}_k^i$ where $\mathbf{p}_{0_k}^{ij} = \mathbf{p}_k^i - \mathbf{s}_k^{ij}\, D_k^{ij}$ denotes the point in the plane closest to $\mathbf{p}_k^i$ and $D_k^{ij} = \mathbf{s}_k^{ij\prime}\, \mathbf{p}_k^i + {}^4s_k^{ij}$ is the distance along $\mathbf{s}_k^{ij}$ between $\mathbf{p}_k^i$ and $\mathbf{p}_{0_k}^{ij}$. Hence, after some algebraic manipulation, the measurement error expression can be written as

$$\mathbf{e}_k^{ij}(R) = H_k^{ij}\, R\, \mathbf{h}_k^i + \mathbf{c}_k^{ij}\ , \tag{2}$$

where $H_k^{ij} = \rho_k^i\, S_k^{ij}\, R_{ins_k}^i$, $\mathbf{h}_k^i = -R_l\, R_{lb}(\alpha_k^i)\, \mathbf{r}(1)$, $\mathbf{c}_k^{ij} = -S_k^{ij}\, R_{ins_k}^i\, \mathbf{b}^i - S_k^{ij}\, \mathbf{p}_{ins_k}^i - {}^4s_k^{ij}\, \mathbf{s}_k^{ij}$ and $S_k^{ij} = \mathbf{s}_k^{ij}\, \mathbf{s}_k^{ij\prime}$. Also, $R \in$ SO(3) is the calibration parameter matrix to be estimated and the known parameters are $H_k^{ij} \in$ M(3,$\mathbb{R}$) and $\mathbf{h}_k^i, \mathbf{c}_k^{ij} \in \mathbb{R}^3$. In addition, the following assumption characterizes the measurement error distribution.

Assumption 1 (Error distribution): The measurement error distribution is assumed to be Gaussian and defined by $p(\mathbf{e}_k^{ij}) = \mathcal{N}\left(\mathbf{0}, (\sigma_k^{ij})^2\, I\right)$.

The calibration problem can be formulated within the scope of the ML estimation theory as that of maximizing the reconstruction error probability function, i. e.

$$R^* = \arg\min_R f(R) \quad , \quad \text{s. t.} \quad R \in \text{SO(3)}\ , \tag{3}$$

$$f(R) = \sum_{i=1}^{n_c} \sum_{\substack{j=1 \\ j\neq i}}^{n_c} \sum_{k=1}^{n_{p_i}} \frac{1}{2\,(\sigma_k^{ij})^2} \left\| \mathbf{e}_k^{ij}(R) \right\|^2 \ . \tag{4}$$

This cost functional can be further simplified if the successive summations are mapped into only one, by computing all the errors for each combination of cloud-to-cloud comparison and, with a slight abuse of notation, defining the new cost functional as

$$f(R) = \sum_{i=1}^{n} \frac{1}{2\, n\, \sigma_i^2}\ \|\mathbf{e}_i(R)\|^2\ , \tag{5}$$

where each $\mathbf{e}_i(R) = H_i\, R\, \mathbf{h}_i + \mathbf{c}_i$ and σ_i for $i = 1, \ldots, n$ is obtained from the previous variables $\mathbf{e}_k^{ij}(R)$ and σ_k^{ij}, for $i, j = 1, \ldots, n_c$, $j \neq i$ and $k = 1, \ldots, n_{p_i}$, using a simple index map. In the functional of Eq. (5), the average of the errors is considered in order to improve the numeric behavior of the algorithm, since the total number of considered points may vary from iteration to iteration. Note that resorting to optimization techniques based on the Newton method, instead of standard nonlinear least squares methods, allows for a more efficient estimation algorithm, as the second order derivative of the cost functional can be used.

III. Optimization on Riemannian Manifolds

This section introduces the optimization methodology on Riemannian manifolds. Since the rotation matrix R is an element of the group of special orthogonal matrices SO(3), which is an embedded submanifold of $M(3, \mathbb{R})$, the optimization tools adopted in this section are based on simple exercises of Riemannian Geometry theory and allow for the minimization of the likelihood function directly on the manifold of special orthogonal matrices SO(3). The concepts of intrinsic gradient and Hessian derived for SO(3) produce descent directions in the manifold and the cost functional is minimized along geodesics in SO(3). For a comprehensive introduction to the subject and for applications with orthogonality constraints the reader is referred to [10], [11].

Considering the log-likelihood function f : SO(3) $\rightarrow \mathbb{R}$ given in (5), the optimization problem reduces to the one defined in (3). The estimate $\hat{R}$ of the optimal value R^* is computed using the Gradient or the Newton methods generalized to manifolds. Given the current parameter estimate R_k, at iteration k, these methods compute a descent direction in the intrinsic tangent space, $\mathbf{d}_k \in T_{R_k}$SO(3), and allow to obtain the new estimate R_{k+1} by solving a minimization subproblem along the geodesic of the manifold, i. e., a line search. This algorithm is structured as Algorithm 1, where $\gamma_{\mathbf{d}_k}(t) \in$ SO(3) is defined as the geodesic of the manifold with initial conditions $\gamma_{\mathbf{d}_k}(0) = R_k$ and $\dot{\gamma}_{\mathbf{d}_k}(0) = \mathbf{d}_k$.

Algorithm 1: Generic minimization algorithm for the LADAR calibration problem:

1) Initialize R_0 and let k = 0;
2) Compute descent direction $\mathbf{d}_k$;
3) Compute the step size by solving the minimization subproblem $t_k^* = \arg\min_{t\geq 0} f\left(\gamma_{\mathbf{d}_k}(t)\right)$;
4) Compute next parameter estimate: $R_{k+1} = \gamma_{\mathbf{d}_k}(t_k^*)$;
5) Test if $\left\|\nabla f|_{R_{k+1}}\right\| < \epsilon$: if true, let $\hat{R} = R_{k+1}$ be the final estimated parameter and stop; if false, let $k \leftarrow k+1$ and go to step 2.

The accuracy of the estimate is determined by the constant ϵ and the norm is determined using the metrics in the parameter space SO(3). Hence, it is necessary to define the metric for the rotation matrix $R \in$ SO(3), which is inherited from the canonical metric in the Euclidean space M(3,$\mathbb{R}$). While the tangent space of M(3,$\mathbb{R}$) is identified with T_RM(3,$\mathbb{R}$) $\simeq$ M(3,$\mathbb{R}$) and represented by the usual gradient, the tangent space of SO(3) at point R is identified by T_RSO(3) $\simeq R$K(3) $= \{R\,K : K \in \text{K(3)}\}$, where K$(n) = \{K \in \text{M}(n, \mathbb{R}) : K = -K'\}$. To define the canonical metric in SO(3), let two tangent vectors $\{\delta_1, \delta_2\} \in T_R$SO(3), which are identified by $\delta_1 \simeq R\,K_1$ and $\delta_2 \simeq R\,K_2$, with $\{K_1, K_2\} \in$ K(3), then $\langle \delta_1, \delta_2 \rangle = \text{tr}\,(\delta_1'\, \delta_2)$, where tr$\,(.)$ stands for the trace of a matrix.

The following three sections address: a) the computation of a descent direction, using both the gradient and the Newton methods, b) the line search algorithm with Wolfe conditions and c) the deterministic line search algorithm that computes an exact step size.

A. Descent Direction

To improve the accuracy of the descent direction estimate, generalizations for manifolds of the Gradient and the Newton methods are adopted. While the former is easier to derive and implement, the Newton method yields very fast convergence near the minimum. The derivation of the gradient and the Hessian of the log-likelihood function are described below specifically for the SO(3) manifold.

1) Gradient Method: The log-likelihood function (5) can be generalized to M(3,$\mathbb{R}$) by defining the smooth function $\hat{f}$: M(3,$\mathbb{R}$) $\rightarrow \mathbb{R}$ such that $\hat{f}|_{\text{SO(3)}} = f$. The tangent space

on M(3,$\mathbb{R}$) is characterized as the direct sum of two tangent spaces complementary to SO(3), that is

$$T_R\text{M(3,}\mathbb{R}) = T_R\text{SO(3)} \oplus (T_R\text{SO(3)})^{\perp} \ , \tag{6}$$

where the operator $\oplus$ stands for the direct sum of two sets and $(T_R\text{SO(3)})^{\perp}$ is the orthogonal complement of T_RSO(3). The smooth vector field defined by the extrinsic gradient $\text{grad}\hat{f}|_R \in T_R\text{M(3,}\mathbb{R})$ is decomposed as the sum of its tangent and orthogonal components

$$\text{grad}\hat{f}|_R = \left(\text{grad}\hat{f}|_R\right)^{\top} + \left(\text{grad}\hat{f}|_R\right)^{\perp} \tag{7}$$

and is identified with the usual gradient in M(3,$\mathbb{R}$), that is

$$\text{grad}\hat{f}|_R \simeq \nabla\hat{f}|_R := \frac{\partial f}{\partial R} := \left[\frac{\partial f}{\partial r_{ij}}\right]_{i,j\in\{1,2,3\}} . \tag{8}$$

Hence, the intrinsic gradient $\nabla f|_R \in RK(3)$ is obtained by the projection of the extrinsic gradient on the tangent space T_RSO(3), i.e. $\nabla f|_R = (\nabla\hat{f}|_R)^{\top}$. The projection of the extrinsic gradient results from an optimization problem with closed solution given by

$$\nabla f|_R = R \arg\min_{K\in\mathcal{K}} \left\|\nabla\hat{f}|_R - RK\right\|^2 = R\text{skew}\left(R'\nabla\hat{f}|_R\right)$$

where $\text{skew}(A) = 1/2\,(A - A')$ is the skew symmetric component of A. The extrinsic gradient expression for the considered cost functional is given by

$$\nabla\hat{f}|_R = \sum_{i=1}^{n} \frac{1}{n\,\sigma_i^2} H_i'\,(H_i\,R\,\mathbf{h}_i + \mathbf{c}_i)\,\mathbf{h}_i' \ . \tag{9}$$

Thus, at each iteration k the intrinsic gradient direction used in the optimization algorithm is $\mathbf{d}_k = -\nabla f|_R$.

2) Newton Method: The Newton method uses the second order properties of the log-likelihood function to compute descent direction. Although this method is harder to compute and requires more memory, the convergence rate is greater near the optimal value than that of the gradient method.

Given two tangent vectors $\{X, Y\} \in T_R$SO(3) and the correspondent extension $\{\hat{X}, \hat{Y}\} \in T_R\text{M(3,}\mathbb{R})$, the intrinsic Hessian is given by compensating the external Hessian

$$\text{Hess}f\,(X, Y) = \text{Hess}\hat{f}\left(\hat{X}, \hat{Y}\right) + \Pi_R\,(X, Y)\,\hat{f} \ , \tag{10}$$

where the second fundamental form $\Pi_R\,(X, Y) : T_R\text{SO(3)} \times T_R\text{SO(3)} \rightarrow (T_R\text{SO(3)})^{\perp}$ is a differentiable local vector field on M(3,$\mathbb{R}$) normal to SO(3). The external Hessian is identified by the usual second order derivative in Euclidean spaces

$$\begin{aligned} \text{Hess}\hat{f}\left(\hat{X}, \hat{Y}\right) &= \text{vec}\,(\mathbf{X})'\ \nabla^2\hat{f}|_R\,\text{vec}\,(\mathbf{Y}) \ , & (11)\\ \nabla^2\hat{f}|_R &= \frac{\partial^2\,\hat{f}}{\partial\text{vec}\,(R)\ \partial\text{vec}\,(R)'} \ , & (12) \end{aligned}$$

where $\hat{X} \simeq \mathbf{X} \in$ M(3,$\mathbb{R}$), $\hat{Y} \simeq \mathbf{Y} \in$ M(3,$\mathbb{R}$) and the $\text{vec}\,(.)$ operator is the vectorization of a matrix. The second fundamental form applied to $\hat{f}$ yields $\Pi_R\,(X, Y)\,\hat{f} = -\langle R\,\text{symm}(X'\,Y), \nabla\hat{f}|_R\rangle$, where $\text{symm}(A) = 1/2\,(A + A')$ is the symmetric component of A, and

$$\nabla^2\hat{f}|_R = \sum_{i=1}^{n} \frac{1}{n\,\sigma_i^2} \mathbf{h}_i\,\mathbf{h}_i' \otimes H_i'\,H_i \ , \tag{13}$$

where $\otimes$ is the Kronecker product operator. The Newton method search direction is the unique tangent vector $\mathbf{d} \in T_R$SO(3) that satisfies $\text{Hess}f\,(X, \mathbf{d}) = -\langle X, \mathbf{d}\rangle$ for all $X \in T_R$SO(3). Let $\varepsilon = \{\mathbf{E}_1, \mathbf{E}_2, \ldots, \mathbf{E}_m\}$ be an orthonormal basis for T_RSO(3), then the Newton direction coordinates z_i in the basis ε, $\mathbf{d} = \sum_{i=1}^{m} z_i\,\mathbf{E}_i$, are computed by solving the linear system $A_{hess}\,\mathbf{z} = \mathbf{b}_{hess}$, where $A_{hess} = \{\text{Hess}f\,(\mathbf{E}_i, \mathbf{E}_j)\}$, $\mathbf{z} = \{z_j\}$ and $\mathbf{b}_{hess} = -\{\langle\mathbf{E}_i, \nabla f|_R\rangle\}$, for $i, j = 1, \ldots, m$.

B. Line Search

A geodesic is defined as the curve in the manifold with zero acceleration, and is fully characterized by its initial position and velocity conditions, $\gamma_d(0)$ and $\dot{\gamma}_d(0)$ respectively. In the particular case of SO(3), the geodesic $\gamma_d : J \rightarrow$ SO(3) is defined as $\gamma_d(t) = R\,e^{R'\,\mathbf{d}\,t}$, where J is an interval in $\mathbb{R}$ and $\mathbf{d} \in RK(3)$ identifies the tangent vector.

The step size optimization subproblem of Algorithm 1 is numerically solved using the Wolfe conditions [12], generalized to line search on geodesics. Consider the function $\phi : \mathbb{R} \rightarrow \mathbb{R}$ defined as $\phi(t) = f\,(\gamma_d(t))$ with derivative given by $\dot{\phi}(t) = \nabla' f|_{\gamma_d(t)}\,\dot{\gamma}_d(t)$ and let also $\mu_k = \phi(0) + \sigma\,\dot{\phi}(0)\,t_k$ and $\mu_0 = \lambda\,\dot{\phi}(0)$, where σ and λ are parameters of the algorithm. The Wolfe rule classifies the step size according to the sets

$$\begin{aligned} \mathcal{A} &= \left\{t_k > 0 : \phi(t_k) \leq \mu_k \ \wedge\ \dot{\phi}(t_k) \geq \mu_0\right\} & (14)\\ \mathcal{D} &= \{t_k > 0 : \phi(t_k) > \mu_k\} & (15)\\ \mathcal{E} &= \left\{t_k > 0 : \phi(t_k) \leq \mu_k \ \wedge\ \dot{\phi}(t_k) < \mu_0\right\} & (16) \end{aligned}$$

that define the acceptable, the right unacceptable and the left unacceptable step sizes, respectively. The line search algorithm consists of finding an acceptable step size, i. e., an estimate of the optimal step size.

C. Deterministic Line Search

Taking advantage of the periodicity of the objective function, the exact optimal solution for line search problem can be found by simply determining the roots of a fourth order polynomial, as detailed in [14], for a similar cost functional. Given a search direction $\mathbf{d}$, computed using either the Gradient or the Newton methods, the line search optimization subproblem is defined by $t^* = \arg\min_{t\geq 0}\,\phi(t)$, where $\phi(t) = f\,(\gamma_d(t))$. To tackle a more general type of optimization problem let the cost functional be written as

$$\begin{aligned} \phi(t) \quad = \quad & \sum_{i=1}^{n} \frac{1}{2\,\sigma_i^2}\,\text{tr}\,\big(M_i'\,e^{-\Omega\,t}\,R'\,N_i\,R\,e^{\Omega\,t}\,M_i \\ & +2\,W_i'\,R\,e^{\Omega\,t}\,M_i + C_i\big) \end{aligned} \tag{17}$$

where $M_i = \mathbf{h}_i$, $N_i = H_i'\,H_i$, $W_i = \mathbf{c}_i'\,H_i$, $C_i = \mathbf{c}_i'\,\mathbf{c}_i$ and $\Omega = \frac{1}{\|\boldsymbol{\omega}\|}[\boldsymbol{\omega}\times]$ with $[\boldsymbol{\omega}\times] = R'\,\mathbf{d}$. The skew-symmetric matrix $[\mathbf{a}\times]$ stands for the cross product operator for vector $\mathbf{a}$. In

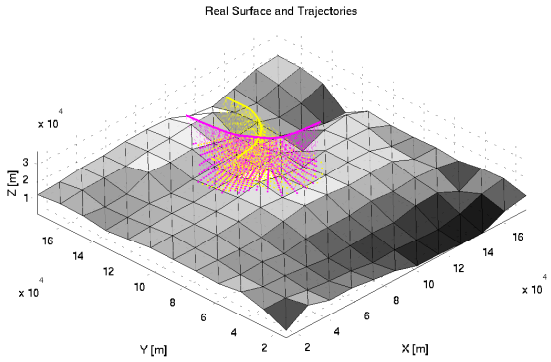

Fig. 2. $\mathcal{S}_{\text{real}}$, trajectories and laser beams

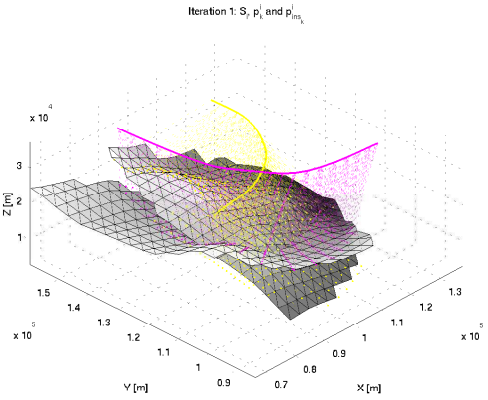

(a) Before Calibration

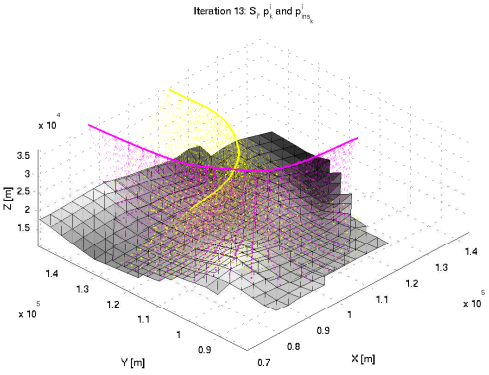

(b) After Calibration

Fig. 3. Calibration example (35×35 aproximations grid): $\mathcal{S}_1$, $\mathcal{S}_2$, trajectories and laser beams

this way Ω has unit length allowing the usage of Rodrigues' formula $e^{\Omega\, t} = I + \Omega \sin t + \Omega^2 (1 - \cos t)$. Substituting this formula into (17) and simplifying, it can be seen that $\phi(t) = k_1 + k_2 \sin t + k_3 \cos t + k_4 \sin 2\, t + k_5 \cos 2\, t$, where $k_j,\ j = 1, \ldots, 5$ are constant scalars. To find the optimal value for the step size the first order condition of optimality, that is $\frac{d\,\phi(t)}{dt} = 0$, yields $k_2 \cos t - k_3 \sin t + 2\, k_4 \cos 2\, t - 2\, k_5 \sin 2\, t = 0$ and the optimization subproblem is now to find the values of $t \in [0, 2\,\pi)$ for which the previous condition is satisfied.

The first step is to make a trigonometric half-angle substitution, i. e., $x = \tan \frac{t}{2}$, reducing the first order condition of optimality to a fourth order polynomial in x, $x^4 + b_3\, x^3 + b_2\, x^2 + b_1\, x + b_0 = 0$, where $b_i,\ i = 0, \ldots, 3$ are constant scalars. After finding the roots of this quartic polynomial, which is a standard procedure [14], the optimal value of t is the real root for which the cost functional is minimal.

IV. Simulation Results

To assess the performance of the proposed algorithms, a low resolution digital elevation map, for the sake of clarity, is used to define the simulated real surface $\mathcal{S}_{\text{real}}$. This can be seen in the example of the calibration setup shown in Fig. 2, where there are two different platform trajectories (in magenta and yellow) and the respective acquired points. In Fig. 3, the two surfaces obtained from the two clouds of laser measured data are shown, considering an erroneous installation matrix. Considering the presented optimization methods and line search algorithms, two different configurations are tested: 1) Riemannian optimization with Wolfe rule and 2) Riemannian optimization using exact step size. These methods are hereafter compared to highlight the advantages and disadvantages of each of them. In both methods, the computation of the search direction is performed using the Newton's method. An error distance that is defined in SO(3) is used to compare the solutions of the different configurations. Let $R^*, \hat{R} \in$ SO(3) be the optimal and the estimated rotation matrices, respectively, and let also $\tilde{R} = \hat{R}'\, R^* \in$ SO(3) be the error matrix, thus, the performance of each method is evaluated by defining the distance from $\tilde{R}$ to I as $\|\tilde{R}\|_{\text{SO(3)}} = \arccos(\frac{1}{2}(\text{tr}(\hat{R}'\, R^*) - 1))$.

The objective of the simulations presented hereafter is to analyse the properties of the calibration algorithm as well as to demonstrate that there is a relation between the number of planes considered for the surface approximation and the solution precision that can be achieved by the optimization method, considering the same number of laser measured points. The surface approximation algorithm is based on a xy-plane uniform sampling grid for each cloud of laser points, and evaluates the best z-coordinate value based on the surrounding laser points. A set of planes is then generated in order to be used by the calibration method in each iteration. To stablish the relation between the number of planes and the solution accuracy, two surface approximation grids are considered: i) a 20×20 grid and ii) 35×35 grid. The simulation experience consisted of 100 Monte Carlo runs for case i) and 14 Monte Carlo runs for case ii), with random initial conditions computed using a uniform distribution between -20 and 20 degrees for each component of the ZYX Euler angle vector $\mathbf{x}_0$ yielding the rotation matrix $R_0 = R(\mathbf{x}_0)$. The optimal value for all the trials is defined by the rotation matrix, $R^* = R(\mathbf{x}^*)$, obtained from the ZYX Euler angles $\mathbf{x}^* = \begin{bmatrix} 0.10 & 0.05 & -0.04 \end{bmatrix}'$. The stopping criterion used was $\frac{\|\nabla f|_R\|}{\|\nabla f|_{R_0}\|} < 10^{-6}$. All the simulations were performed using Matlab on an Intel Pentium Core 2 Duo processor at 2.66 GHz.

Table I presents the statistical indicators of the simulation

TABLE I

SUMMARY OF RESULTS.

	Surface Approximation Grid		
	20×20	35×35	Method
Average Computation Time [hour]	0.673	2.252	1
	0.672	2.176	2
Average Number of Iterations	16.1	10.23	1
	15.4	9.538	2
Average Distance to Optimal [rad]	0.011847	0.006634	1
	0.011282	0.006583	2
Maximum Distance to Optimal [rad]	0.013803	0.008293	1
	0.013803	0.008292	2
Number of runs	100	14	

described above: the average computation time, the number of iterations, the average and maximum distances in SO(3) to the optimal solution. From these indicators, no obvious difference can be observed in the computational time and iteration number, when comparing the two methods. Nevertheless, it seams that method 2, which uses the exact step computation, achieves better values in these two indicators. With respect to the average and maximum distance to the optimal solution, the differences between the two methods is almost negligeble, yet, method 2 achieves the best values in every indicator for both the 20×20 and the 35×35 approximation grids. The main conclusion emerging from this simulation results is that there is an obvious relation between the accuracy of the obtained solutions and the surface approximation used in the methods, noting that increasing the surface approximation grid from 20×20 to a 35×35 grid, decreased the distance to the optimal solution by 44.0% in the case of method 1 and by 41.7% in the case of method 2. Similar decreasing factors were obtained for the maximum distance to the optimal solution. Moreover, the accuracy obtained using the 35×35 approximation grid, less than 0.0067 radians, indicates that the proposed calibration method can achieve good accuracy calibration of the laser instalation matrix, specially if more accurate surface approximations are considered.

The comparison between the approach presented in [8] and the new method presented here is unfair and difficult, since the former consideres a known calibration surface in order to compare the acquired data and the noise conditions are different. Nonetheless, it can be observed that the average distance to the optimal solution of the new method is always below those of the method presented in [8] when noise is considered, which achieves the values 0.019 rad and 0.016 rad for algorithms 1) and 2), respectively.

V. CONCLUSIONS

This paper addresses the problem of automatic LADAR calibration by proposing numerical optimization methods, that estimate the mounting bias rotation matrix $R \in \mathrm{SO}(3)$. This id achieved by minimizing the distances between several clouds of acquired laser points, without any knowledge of the terrain. The optimization methods are based on a the generalization of the Newton method to SO(3), estimating the mounting bias rotation matrix, and both the Wolfe rule and a deterministic method are used for the computation of the step size. These methods and compared and analyzed in simulation.

The main contribution of this work is to suppress the use of a control surface, which represents the true terrain and to which all measured points are compared in the literature. Instead, the proposed method compares each cloud of points with a surface approximation of the remaining clouds. The performance and limitations of the calibration method was extensively tested in Matlab and the results indicate that the proposed algorithm is able to find good estimates for the laser calibration problem. Additionally, the accuracy of these estimates is shown to increase with the number of planes used to describe surface approximation of each cloud of laser measured points.

One future direction of research is to consider nonuniform surface approximations in order to decrease the computational time, as the same approximation error might be achieved with less planes. Further work is also needed in order to include other sources of reconstruction errors, like the time delay between laser acquisition and the INS/GPS data or the range measurement error.

REFERENCES

[1] W. B. Krabill, R. H. Thomas, C. F. Martin, R. N. Swift, and E. B. Frederick, "Accuracy of airborne laser altimetry over the greenland ice sheet," *International Journal of Remote Sensing*, vol. 16, no. 7, pp. 1211–1222, 1995.

[2] E. Næsset and T. Økland, "Estimating tree height and tree crown properties using airborne scanning laser in a boreal nature reserve," *Remote Sensing of Environment*, vol. 79, no. 1, pp. 105–115, January 2002.

[3] S. Thrun, M. Diel, and D. Hähnel, "Scan alignment and 3-d surface modeling with a helicopter platform," in *Proceedings of the 4th International Conference on Field and Service Robotics*, July 2003.

[4] R. Madhavan and E. Messina, "Iterative registration of 3d ladar data for autonomous navigation," in *Intelligent Vehicles Symposium, 2003. Proceedings.* IEEE, June 2003, pp. 186–191.

[5] J. R. Ridgway, J. Minster, N. Williams, J. L. Bufton, and W. B. Krabill, "Airborne laser altimeter survey of long valley, california," *Geophysical Journal International*, vol. 131, no. 2, pp. 267–280, November 1997.

[6] A. Habib and T. Schenk, "A new approach for matching surfaces from laser scanners and optical sensors," in *International Archives of Photogrametry and Remote Sensing*, ser. Part 3 W14, vol. 32, 1999.

[7] S. Filin, "Recovery of systematic biases in laser altimeters using natural surfaces," in *International Archives of Photogrametry and Remote Sensing*, ser. Part 3 W3, vol. 34, 2001.

[8] B. Guerreiro, C. Silvestre, P. Oliveira, and J. F. Vasconcelos, "Nonlinear and geometric optimization techniques for ladar calibration," in *Proceedings of the IEEE International Conference on Robotics and Automation*, Passadena, CA, USA, May 2008, pp. 1406–1411.

[9] S. M. Kay, *Fundamentals of Statistical Signal Processing: Estimation Theory*. Upper Saddle River, New Jersey: Prentice-Hall, Inc., 1993.

[10] A. Edelman, T. A. Arias, and S. T. Smith, "Geometry of algorithms with orthogonality constraints," *SIAM Journal on Matrix Analysis and Aplications*, vol. 20, no. 2, pp. 303–353, 1998.

[11] P. A. Absil, R. Mahony, and R. Sepulchre, *Optimization Algorithms on Matrix Manifolds*. Princeton University Press, 2007.

[12] J. Nocedal and S. Wright, *Numerical Optimization*, ser. Springer Series in Operation Reasearch. Springer, 1999.

[13] F. C. Park, J. Kim, and C. Kee, "Geometric descent algorithms for attitude determination using the global positioning system," *AIAA Journal of Guidance, Control and Dynamics*, vol. 23, no. 1, pp. 26–33, January-February 2000.

[14] M. Abramowitz and I. A. Stegun, *Handbook of Mathematical Functions with Formulas, Graphs, and Mathematical Tables*. New York: Dover Publications, 1972.